# IMPACT OF WANING IMMUNITY AND RELAPSE ON THE EFFECTIVE REPRODUCTION NUMBER IN TUBERCULOSIS TRANSMISSION: A SENSITIVITY ANALYSIS

**Ogunmodimu, M. O., Yusuf, T. T., Olotu, O. O. and Olabode, B. T.**


DOI10.51459/jostir.2026.2.1.0100

Department of Mathematical Sciences, School of Physical Sciences, The Federal University of Technology, Akure, P.M.B. 704, Akure, Ondo State, Nigeria

**Correspondence**
akinademary18@gmail.com

**History**
**Received: 24-07-2025**
**Accepted: 23-10-2025**
**Published: April, 2026**

## ABSTRACT

It was approximated that one-third of the world's population is infected with latent Tuberculosis (TB). Moreover, the emergent prevalence of Covid-19 resulted in a drastic decline of treatment and diagnosis of TB. This research presented an exhaustive deterministic model for the transmission, prevention and control dynamics of TB. The developed model incorporated significant epidemiological factors such as disease relapse, progression rate from latent to active TB, contact rate, treatment rate, vaccination and immunity wane. The model was shown to possess a positive and bounded solution region. By employing the next generation matrix technique and constructing an appropriate Lyapunov function respectively, it was obtained that there exists a locally and globally stable disease free equilibrium point for the model whenever the effective reproduction number, $R_e$, is less than unity. Similarly, the model was shown to possess a unique globally asymptotically stable endemic equilibrium point (EEP) whenever $R_e > 1$. Sensitivity analysis of $R_e$ was performed using the forward index sensitivity approach and it was established therein that the rate of recruitment into the susceptible population and the disease transmission rate have unit sensitivity indices. Rates of immunity wane after vaccination and progression from latent to active TB exhibited a direct variation while vaccination, treatment, natural and disease induced death rates exhibited an inverse variation with $R_e$. Numerical simulation was performed on the model by implementing the fourth order Runge Kutta numerical method on MATLAB subroutine. The data used for simulation was gotten from literature and referenced. The values of the model's sensitive parameters were varied and their effects on the spread and control of TB were discussed extensively.

**Keywords:** Mathematical Model, Disease Relapse, Sensitivity Analysis, Tuberculosis, Waning Immunity.

## 1. | Introduction

"Following three years in which COVID-19 was the leading cause of death from infectious diseases, Tuberculosis (TB) reclaimed this position in 2023 with an estimate of 1.25 million deaths" (Goletti *et al.,* 2025). Tuberculosis is an infectious disease caused by the bacillus mycobacterium tuberculosis (MTB). TB typically attacks the lungs (pulmonary TB) but can also affect other body parts (extra-pulmonary TB) such as the central nervous system, lymphatic system, brain, spine, kidneys of people with weak immune systems and young children (Kim *et al.,* 2018). TB infection dates as far back as 1882 when Dr. Robert Koch made known the discovery of tubercle bacilli, later known as the MTB, a pathogenic

https://www.futa.edu.ng

JOSTIR
JOURNAL OF SCIENCE, TECHNOLOGY AND INNOVATION RESEARCH
https://jostir.futa.edu.ng

bacterial specie of the mycobacterium species and the causative agent of most cases of tuberculosis (Patterson *et al.,* 2018). In the medical writings of Europe, the terms phthisis, consumption and white plague were once used as synonym for TB (Frith, 2014).

TB is transmitted through airborne particles known as droplet nuclei which is generated when an already infected person discharges fluid via coughing, sneezing, shouting, singing etc. These nuclei are sufficiently small to remain suspended in the air and carried throughout rooms or buildings by normal air currents. Individuals who continuously share space with someone infected with TB have a high risk of becoming infected. These bacilli establish themselves in the alveoli of the lungs, from which they disseminate throughout the body except suppressed by a strong immune system.

A person is said to be exposed to TB when they breathe in tubercle bacilli from contaminated air space, although at this early stage such person is non-infectious and asymptomatic (latent TB). While it is estimated that one-third of the world's population are infected with latent TB, only approximately 10% of latent progress to active/clinical infectiousness (Centers for Disease Control and Prevention, 2024). These include people who have a weak immune system or are infected with other diseases such as Covid-19. In such person, the bacteria become active, replicate, and lead to the development of TB disease. For those who do not develop active TB, the bacteria remain inactive (latent) for a lifetime in them. Those who develop TB usually do so within the first two years of infection.

The World Health Organization (WHO) declared TB as a global epidemic in 1993 (Mishra and Srivastava, 2014). More than 80% of global TB incidence is concentrated in 23 countries across East Asia and Africa with TB accounting for 3 million deaths worldwide yearly and at least one billion deaths during the 19th and early 20th centuries (Castillo-Chavez and Song, 2004). "TB is the 10th leading cause of death worldwide since 2007 and the main cause of death globally from a single infectious agent, ranking above HIV/AIDS" (Schluter *et al.,* 2021).

TB is treated with multiple antibiotics, including combination of Streptomycin and pyrazinamide over a period (Grace *et al.,* 2019). Individuals at the latent stage are treated with isoniazid for at least 6 months for effective results while active cases are treated for at least 9 months with multiple drugs including rifampin, isoniazid, pyrazinamide and complex regimens. Individuals with active disease may recover if they are treated with timely and appropriate antibiotic regimens, although they remain at risk of a disease relapse (Colijn *et al.,* 2009). Antibiotic resistant TB strains are generated when there is a wrong diagnosis/therapy, a co-infection with another disease(s), an incomplete treatment or skipped dose(s). Antibiotic resistance continues to intensify, accompanied by increasing levels of multidrug-resistant TB. Antibiotics are effective for treating drug-sensitive TB, but drug-resistant TB is much harder to manage, and sometimes impossible to treat (Kirschner *et al.,* 2017).

Moreover, treatment of a TB infected individual does not remove tubercle bacilli, the causative agent. Recovered individuals are categorized as a single low-risk latent group who can get re-infected due to loss of immunity. Individuals at the active stage of TB infectiousness, if not immediately treated, are at a risk of death. Unavailability of early and accurate diagnosis are two major obstacles to TB control efforts in high-burden countries. Although sputum smear microscopy is the standard TB diagnostic method across the world, it detects only about 50% of active TB cases in most laboratories. Bacillus Calmette-Guerin (BCG) vaccine has a good efficacy in preventing TB disease in the years after vaccination. This immunity, however, may be lost by continuous exposure to a significantly endemic environment (Okafor *et al.,* 2023). Therefore,

vaccination is not a ticket to continuous exposure to the infection especially in a highly endemic environment such as developing countries.

Figure 1 illustrates global TB treatment numbers between 2010 and 2022, showing substantial reversals in progress toward increasing annual diagnoses and treatment in 2020 and 2021. This is caused by the emergent prevalence and chaotic spread of Covid-19 (Bandekar and Ghosh, 2022) and results in substantial disruption of progress toward global TB treatment goals (Sachdeva *et. al*., 2020; World Health Organization, 2023).

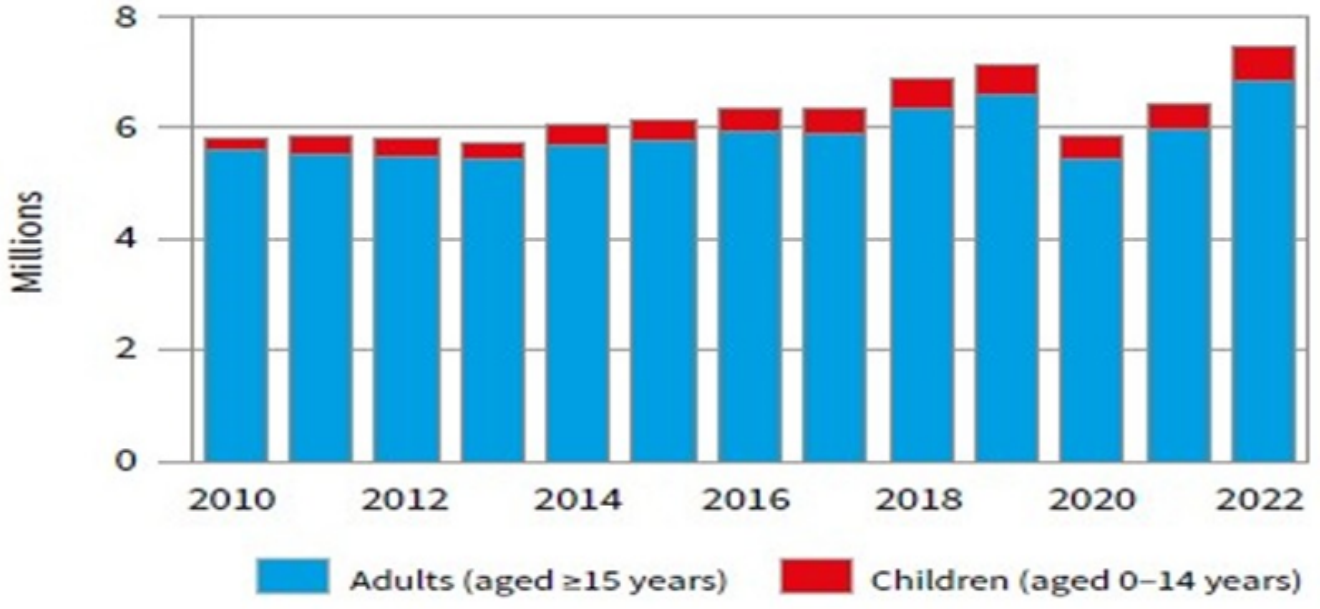


**Figure 1 |** The Global Number of People treated for TB Disease, 2010–2022 (World Health Organization, 2023)

## 2. | Literature Review

The strategic application of mathematical modelling enables the identification of high-impact interventions and the optimal allocation of limited resources (Mandal *et al.,* 2025). Waaler *et al.* (1962) developed one of the earliest mathematical models on TB dynamic, with focus on its prediction and control using simulation approaches. Three epidemiological classes were included in the model: susceptible, latent TB, and infectious TB. In the model formulation, it was assumed that BCG vaccine prevented 70% of possible TB infection from taking place among the vaccinated population. Measures of disease burden such as TB mortality, prevalence, and incidence were also considered in the model formulation. The model was solved using observed or estimated epidemiological data from the Frimodt-Moller's longitudinal survey in South India. Graphical representations of the results showed the effects of BCG vaccines, case finding and treatment on the prevalence of the infection over a period of 20 years. This research was also used to forecast the future course of TB under specific conditions. Subsequent mathematical research on TB focuses not only on simulation of models but also on their dynamical analysis using modern and more advanced mathematical methods.

White and Abubakar (2016); Abu-Raddad *et al.* (2009); Wu *et al.* (2010); Ayinla *et al.* (2021); Koriko and Yusuf (2008) presented the impacts of mathematical modeling in understanding and controlling TB infection. Mathematical models were described as effective for; gaining insight into TB's history, for evaluating "what ifs" scenarios, examining the impacts of interventions that have/ have not yet been implemented, analyzing empirical data and to integrate evidence from different sources. The use of mathematical models to examine

observational study data when trials are impracticable was described as very significant to gaining effective public health intervention strategies.

Trauer *et al.* (2014) developed a 10-compartment TB model, taking into cognizance the multidrug resistant TB and de novo resistance arising during treatment. Sensitivity analysis of the model indicated that the detection and treatment rates of all infected individuals, irrespective of the strain, are the key parameters influencing subsequent disease incidence and in predicting the population-wide mortality. A similar result was obtained by Ayinla *et al.* (2021) using a 7-compartmental model to describe the Tuberculosis dynamics. Vaccination program, patients' diagnosis and treatment of patient were identified as the most important measures in attaining an effective TB control with diagnosis been the most preferred measure.

Pandey *et al.* (2017) predicted the incidence of TB yearly in India stratified into urban and rural areas. The result of the developed model's simulation indicated that TB in urban areas is unique for infecting more new individuals yearly (i.e., high rate of infection) due to high contact rate amongst the population while TB in rural areas is driven by a large prevalent pool (a single case remaining infectious for a considerably long period) traceable to limited access to treatment. It was also observed that the average duration of infectiousness depended mainly on mortality, spontaneous recovery and cure through diagnosis and treatment. Owolabi and Pindza (2022) developed a nonlinear model of TB dynamics with control measures. The existence–uniqueness properties of the model solution were established and numerical analyses performed for a range of control and fractional-order parameter values. The study concluded that reductions in TB incidence and mortality depend on the efforts of national governments to implement appropriate control measures.

Despite the significance of the studies presented in modeling the dynamics of Tuberculosis, substantial focus hasn't been directed toward the effect of reinfections due to disease relapse and waning immunity especially post-vaccination. Similarly, the re-emergence of Covid-19 led to a rapid decline in the treatment and diagnosis of TB. Both tuberculosis and SARS-CoV-2 target the respiratory tract including the lungs, thus potentiating their effect on each other and mutually accelerating there progression to a critical stage (Schluter *et al.,* 2021). Moreover, Covid-19 patients are predisposed to aggravated activation of latent infection or occurrence of new infection with TB due to their weakened immune system, similar to opportunistic infections in the case of HIV/AIDS (Ogunmodimu *et al.,* 2024). It is therefore imperative to develop a model that incorporates these factors into the TB dynamic. This work addressed that gap by constructing an exhaustive deterministic model that considers both waning immunity and reinfection dynamics due to disease relapse.

## 3. | Development of the Model

For the development of the TB model, we employed the compartmental disease modeling approach. The total human population was defined as $N_T(t)$ and classified into 5 mutually exclusive time-dependent disease-status based compartment. The susceptible population $S(t)$ comprise of individuals who live within a TB endemic population but are not (yet) infected with TB nor are vaccinated against it at time $t$; the latent TB infected population $I_L(t)$ are individuals who have a latent TB infection; the active TB infected population $I_A(t)$ are individuals who have an active TB infection; the recovered population $R_T(t)$ are individuals who recovered from TB via treatment while the vaccinated population $V_T(t)$ are individuals who have been vaccinated against TB.

Individuals are migrate into the susceptible population at the rate $\Lambda$ while the natural death

rate of all individuals in the studied population is denoted by $\mu$. The TB induced death rate is $\delta_T$ while the transmission rate of TB is $\beta_T$. Individuals in the susceptible and vaccinated populations can contract TB by contact with the infected population, $I_A$, via the force of infection $\lambda_T = \beta_T I_A$. The TB vaccination and recovery rates are $\nu_T$ and $\gamma_T$ respectively. The rates of loss of immunity for the vaccinated population and disease relapse for the recovered population are denoted respectively by $\omega_T$ and $\theta_T$. $\rho_1$ denotes the transition rate from latent to active TB. Figure 2 shows the flow diagram for the developed model while Table 1 contains its state variables.

**Table 1** | The Model's State Variables

| Variables | Description |
|---|---|
| $S(t)$ | Susceptible Population |
| $I_L(t)$ | Latent TB Infected Population |
| $I_A(t)$ | Active TB Infected Population |
| $R_T(t)$ | TB Recovered Population |
| $V_T(t)$ | TB Vaccinated Population |

### 3.1 | The TB Model

$$\frac{dS}{dt} = \Lambda - \nu_T S - \lambda_T S + \omega_T V_T + \theta_T R_T - \mu \quad (1)$$

$$\frac{dI_L}{dt} = \lambda_T S - \rho_1 I_L - \mu I_L, \quad (2)$$

$$\frac{dI_A}{dt} = \rho_1 I_L - \gamma_T I_A - (\delta_T + \mu) I_A, \quad (3)$$

$$\frac{dR_T}{dt} = \gamma_T I_A - \theta_T R_T - \mu R_T, \quad (4)$$

$$\frac{dV_T}{dt} = \nu_T S - \omega_T V_T - \mu V_T. \quad (5)$$

satisfying the initial conditions;

$$\left\{ \begin{matrix} S, I_L, I_A, R_T, V_T \in R_+^5 : S_0 > 0, & I_{L0} > \\ 0, & I_{A0} > 0, \quad R_{T0} \geq 0, \quad V_{T0} \geq 0 \end{matrix} \right\}$$

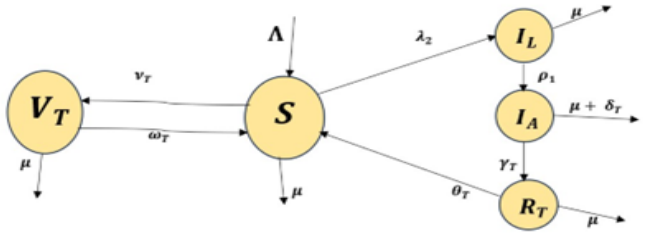


**Figure 2** | Flow Diagram for the Tuberculosis Model

### 3.2 | Qualitative Properties of the Model

To establish the model's epidemiological plausibility, we presented two basic qualitative properties for it. These include identifying the model's invariant region, a set inside which it is bounded, and establishing the positivity of its solution (Lofberg, 2004).

#### *3.2.1 | Boundedness of Solution*

To derive the model's invariant region, the total human population is defined by:

$$N(t) = S(t) + I_L(t) + I_A(t) + R_T(t) + V_T(t) \quad (6)$$

$$\begin{aligned} \frac{dN_T(t)}{dt} &= \Lambda - \mu N_T(t) - \delta_T I_A \\ &\leq \Lambda - \mu N(t) \end{aligned} \quad (7)$$

$$\begin{aligned} &\ln(\Lambda - \mu N(t)) \geq -(\mu t + C) \\ &\implies (\Lambda - \mu N(t)) \geq A e^{-\mu t}, \end{aligned} \quad (8)$$

where $A = e^{-C}$ is a constant.

$$\implies N_T(t) \to \frac{\Lambda}{\mu} \ as \ t \to \infty$$

Therefore, the solution set of the model equations enters and stays inside the region:

$$\Omega = \{(S, I_L, I_A, R_T, V_T) \in R_+^5 : N_T(t) \leq \frac{\Lambda}{\mu}\} \quad (9)$$

#### *3.2.2 | Positivity of the Solution*

The Positivity Theorem (Tilahun *et al.,* 2018): The solutions of a model's equations are positively invariant for future time if the respective initial values of the model's state variables are all non-negative". Let $\Omega_1 = \{(S, I_L, I_A, R_T, V_T) \in R_+^5 : (S_0 \geq 0, I_{L0} \geq 0, I_{A0} \geq 0, R_{T0} \geq 0, V_{T0} \geq 0)\}$, the solution of $(S, I_L, I_A, R_T, V_T)\}$ are non-negative for $t > 0$.

Proof: From equation (1),

$$\frac{dS}{dt} = \Lambda - \nu_T S - \lambda_T S + \omega_T V_T + \theta_T R_T - \mu S$$

$$\geq -(\nu_T + \lambda_T + \mu)S.$$
$$\int \frac{dS}{S} \geq -\int (\nu_T + \lambda_T + \mu)dt$$
$$\ln S(t) \geq -A(t) + C$$
$$S(t) \geq Be^{-A(t)},$$

where $A(t) = (\nu_T + \lambda_T + \mu)dt$, where C denotes an integration constant.

At $t = 0$, $S_0 > 0$,

$\therefore S(t = 0) = S_0 \geq B.$

$S(t) \geq S_0 e^{-A(t)}$ (10)

$\geq 0 \ \forall \ t > 0.$

From equation (2),

$$\frac{dI_L}{dt} = \lambda_T S - \rho_1 I_L - \mu I_I$$
$$\geq -(\rho_1 + \mu)I_L.$$
$$\int \frac{dI_L}{I_L} \geq -\int (\rho_1 + \mu)dt$$
$$\ln I_L(t) \geq -A(t) + C$$
$$I_L(t) \geq Be^{-A(t)},$$

where $A(t) = {}^{R}(\rho_1 + \mu)dt$, where C represents an integration constant and $B = e^C$.

At $t = 0, I_{L0} > 0$

$\therefore I_L(t = 0) = I_{L0} \geq B.$

Accordingly.

$I_L(t) \geq I_{L0}e^{-A(t}$ (11)

$\geq 0 \quad \forall \ t > 0.$

The same results are obtainable for equations (3) to (5).

## 4. | Stability Analyses of Model Equilibrium Points

### 4.1 | The Disease-Free Equilibrium (DFE)

We define the DFE as a solution to the model wherein no individual in the population is infected, as:

$E_{T0} = (S^*, 0, 0, 0, V_T^*)$

satisfying $\frac{dS}{dt} = \frac{dI_L}{dt} = \frac{dI_A}{dt} = \frac{dR_T}{dt} = \frac{dV_T}{dt} = 0$ and $I_L = I_A = R_T = 0$.

Setting equations (1) to (5) to 0, we substitute $I_L = I_A = R_T = 0$, and have;

$$\frac{dS}{dt} = \Lambda - \nu_T S + \omega_T V_T + \theta_T R_T - \mu S = 0, \quad (12)$$
$$\frac{dV_T}{dt} = \nu_T S - \omega_T V_T - \mu V_T = 0. \quad (13)$$

The addition of equations (12) and (13) yields:

$$V_T = \frac{1}{\mu}(\Lambda - \mu S). \quad (14)$$

Substituting (14) in (12) yields:

$$\Lambda - (\nu_T + \mu + \omega_T)S + \Lambda\frac{\omega_T}{\mu} = 0$$
$$\implies S^* = \frac{\Lambda}{\mu}K, \quad (15)$$

where

$$K = \frac{(\mu + \omega_T)}{(\mu + \omega_T + \nu_T)}. \quad (16)$$

Substituting (15) in (14), we have; $V_T^* = \frac{\Lambda}{\mu}K^*$, where $K^* = (1 - K)$

Therefore,

$$E_{T0} = (\frac{\Lambda}{\mu}K, 0, 0, 0, \frac{\Lambda}{\mu}K^*) \quad (17)$$

Note that, $S^* = \frac{\Lambda}{\mu}$ iff $K = 1$ and this $\Rightarrow \nu_T = 0$ and $V_T = 0$.

### 4.2 | Local Stability Analysis of the DFE

In epidemiology, to evaluate the local asymptotic stability of the DFE, the next-generation matrix method is applied by examining the basic

reproduction number, $R_0$. $R_0$ is defined as the mean value of the secondary cases generated by a typical primary case in a fully susceptible population. The method was given and revised by Diekmann *et al.,* (1990); Van-den-Driessche and Watmough (2002) respectively and have been employed by several authors (Baba *et al.,* 2021; Akinade *et al.,* 2019; Akinade and Afolabi, 2020; Ogunmodimu *et al.,* 2024). For a population that is not entirely susceptible, like in our model where there exists a vaccinated class, we obtain, instead, the effective reproduction number, $R_e = R_0X$, where X is the fraction of the population that is susceptible. If the effective reproduction number $R_e < 1$, then the DFE is locally asymptotically stable and unstable otherwise.

The basic reproduction number is defined as the spectral radius of the system's next-generation matrix $FV^{-1}$. We defined the rate at which new infections appear in class $i$, $f_i$, and the rate of transfer of individuals into compartments $i$, $v_i$, in the model equations (1) to (5) as: $f_i = \begin{pmatrix} \beta_T I_A S^* \\ 0 \end{pmatrix}$ and $v_i = \begin{pmatrix} (\rho_1+\mu)I_L \\ (\gamma_T+\delta_T+\mu)I_A - \rho_1 I_L \end{pmatrix}$ where,

$$f_i - v_i = \begin{pmatrix} I_{L'} \\ I_{A'} \end{pmatrix} = \begin{pmatrix} \beta_T I_A S^* - (\rho_1+\mu)I_L \\ \rho_1 I_L - (\gamma_T+\delta_T+\mu)I_A \end{pmatrix}$$

Therefore, $F = \begin{pmatrix} 0 & \beta_T S^* \\ 0 & 0 \end{pmatrix}$ and

$$V = \begin{pmatrix} (\rho_1+\mu) & 0 \\ -\rho_1 & (\gamma_T+\delta_T+\mu) \end{pmatrix}$$

$$\lambda_T = \left[0, \frac{\beta_T S^* \rho_1}{(\delta_T+\gamma_T+\mu)(\rho_1+\mu)}\right], \begin{pmatrix} \frac{\beta_T S^* \rho_1}{(\mu+\rho_1)} & \frac{S\beta_T}{\delta_T+\gamma_T+\mu} \\ 0 & \end{pmatrix} \text{ eigenvalues}$$

$$\therefore R_0^T = \frac{\beta_T S^* \rho_1}{(\delta_T+\gamma_T+\mu)(\rho_1+\mu)}.$$

By substituting the parameter values from table 2 in $R_0^T$, we obtained; $R_e = R_0^T X = 0.0342992217681256$, where X, the percentage of the population that is susceptible to TB is $\frac{4}{10}$. Accordingly, the model's DFE is stable. Table 2 contains the secondary data used for the model analyses and simulations.

Table 2 | Table of the Parameter Values

| Parameters | Values | Sources |
|---|---|---|
| $\Lambda$ | 0.00315 | Rwezaura *et al.* (2022) |
| $\mu$ | 0.0003821 | Rwezaura *et al.* (2022) |
| $\delta T$ | 0.1060 | Jajarmi *et al.* (2019) |
| $\beta_T$ | 0.006 | Mekonen and Obsu (2022) |
| $v_T$ | 0.50 | Rwezaura *et al.* (2022) |
| $\gamma_T$ | 0.516 | Mekonen and Obsu (2022) |
| $\omega_T$ | 0.02 | Rwezaura *et al.* (2022) |
| $\theta_T$ | 0.0005 | Bandekar and Ghosh (2022) |
| $\rho_1$ | 0.020 | Colijn *et al.* (2009) |

### 4.3 | Global Stability Analysis of the DFE Point

Here, we employed the generalized method of constructing Lyapunov functions given by Yusuf (2021). Define $V_T(t,S,I_L,I_A,R_T,V_T) = C_1I_L + C_2I_A$; $C_1,C_2 > 0$.

$$\begin{aligned} \frac{dV_T}{dt} &= C_1I_L' + C_2I_A' \\ &= C_1(\beta_T I_A S - (\rho_1+\mu)I_L) + C_2(\rho_1 I_L - (\gamma_T+\delta_T+\mu)I_A) \\ &= (C_1\beta_T S - C_2(\gamma_T+\delta_T+\mu))I_A + (C_2\rho_1 - C_1(\rho_1+\mu))I_L. \end{aligned} \quad (18)$$

Substituting $C_1 = \frac{\rho_1}{\rho_1+\mu}$ and $C_2 = 1$ in (18), we obtained;

$$V_T' = \left(\frac{\rho_1}{(\rho_1+\mu)}\beta_T S - (\gamma_T+\delta_T+\mu)\right)I_A$$

$$< 0.$$

$$R_0^T < 1 \implies \frac{\rho_1}{(\rho_1+\mu)}\beta_T S - (\gamma_T+\delta_T+\mu) < 0;\ V_T' = 0 \text{ iff } I_A = 0.$$

Therefore, the function $V_T$ is strictly Lyapunov at the DFE point according to the "LaSalle's invariance principle" (La-Salle, 1976) and hence $E_0^T$ is globally asymptotically stable.

### 4.4 | The Endemic Equilibrium Point (EEP) of the Model

An EEP of a disease is defined as a "positive steady state solution in which the disease persists in the studied population" (Brown *et al.,* 2006). A unique EEP was obtained for the model by solving for all its state variables while equating their derivatives with

respect to time to zero. ET* = (S*,IL*,IA* ,RT* ,VT*), are positive state solutions of the model satisfying: $\frac{dS}{dt} = \frac{dI_L}{dt} = \frac{dI_A}{dt} = \frac{dR_T}{dt} = \frac{dV_T}{dt} = 0$. That is;

$$\frac{dS}{dt} = \Lambda - \nu_T S - \beta_T I_A S + \omega_T V_T + \theta_T R_T - \mu S = 0, \quad (19)$$

$$\frac{dI_L}{dt} = \beta_T I_A S - \rho_1 I_L - \mu I_L = 0, \quad (20)$$

$$\frac{dI_A}{dt} = \rho_1 I_L - \gamma_T I_A - (\delta_T + \mu) I_A = 0, \quad (21)$$

$$\frac{dR_T}{dt} = \gamma_T I_A - \theta_T R_T - \mu R_T = 0, \quad (22)$$

$$\frac{dV_T}{dt} = \nu_T S - \omega_T V_T - \mu V_T = 0. \quad (23)$$

From (21),

$$I_A = \frac{\rho_1}{(\gamma_T + \delta_T + \mu)} I_L. \quad (24)$$

Substituting (24) in (20), we have;

$$S^* = \frac{(\rho_1 + \mu)(\gamma_T + \delta_T + \mu)}{\beta_T \rho_1} > 0. \quad (25)$$

From (23), we have;

$$V_T = \frac{\nu_T S}{(\omega_T + \mu)}. \quad (26)$$

Substituting (25) in (26), we have;

$$V_T^* = \frac{\nu_T S^*}{(\omega_T + \mu)} = \frac{\nu_T (\rho_1 + \mu)(\gamma_T + \delta_T + \mu)}{\beta_T \rho_1 (\omega_T + \mu)} > 0. \quad (27)$$

From (21) and (22), we obtain respectively;

$$I_L = \frac{(\gamma_T + \delta_T + \mu)}{\rho_1} I_A, \quad (28)$$

$$R_T = \frac{\gamma_T}{(\theta_T + \mu)} I_A. \quad (29)$$

Adding (19) to (23), we have;

$$\Lambda - \mu S - \mu I_L - (\delta_T + \mu) I_A - \mu R_T - \mu V_T = 0. \quad (30)$$

Substituting (27) to (29) in (30), we have;

$$\Lambda - \mu S^* - \frac{\mu(\gamma_T + \delta_T + \mu)}{\rho_1} I_A - (\delta_T + \mu) I_A - \frac{\mu \gamma_T}{(\theta_T + \mu)} I_A - \frac{\mu \nu_T}{(\omega_T + \mu)} S^* = 0 \quad (31)$$

$$\Lambda - \mu S^* \left(1 + \frac{\nu_T}{(\omega_T + \mu)}\right) = \Lambda - \mu S^* \left(\frac{\omega_T + \nu_T + \mu}{\omega_T + \mu}\right) = A I_A.$$

Where $A = \left[\frac{\mu(\gamma_T + \delta_T + \mu)}{\rho_1} + (\delta_T + \mu) + \frac{\mu \gamma_T}{(\theta_T + \mu)}\right] > 0.$

Therefore,

$$I_A^* = \frac{\Lambda - \frac{\mu S^*}{K}}{A}. \quad (32)$$

Recall $K = \frac{\mu + \omega_T}{\mu + \omega_T + \nu_T}$ from (16).

Therefore, substituting (32) in (28) and (29) respectively, we obtain;

$$I_L^* = \frac{(\gamma_T + \delta_T + \mu)}{\rho_1} I_A^*, \quad (33)$$

$$R_T^* = \frac{\gamma_T}{(\theta_T + \mu)} I_A^*. \quad (34)$$

The last three expressions are positive if $\Lambda - \frac{\mu S^*}{K} > 0$,

$$\frac{\Lambda K}{\mu S^*} = \frac{\frac{\Lambda}{\mu} K \beta_T \rho_1}{(\delta_T + \gamma_T + \mu)(\rho_1 + \mu)} > 1.$$

Therefore, a unique EEP, $E_T^* = (S^*, I_L^*, I_A^*, R_T^*, V_T^*)$, for the TB model exists whenever $R_0^T = \frac{\Lambda K \beta_T \rho_1}{\mu(\delta_T + \gamma_T + \mu)(\mu + \rho_1)} > 1$.

### 4.5 | Global Stability of the EEP

Here, we defined an appropriate Lyapunov function for the TB model at $E_T^*$ as:

$$L_T(S, I_L, I_A, R_T, V_T) = \frac{1}{2}[(S - S^*) + (I_L - I_L^*) + (I_A - I_A^*) + (R_T - R_T^*) + (V_T - V_T^*)]^2 \quad (35)$$

$$\frac{dL_T}{dt} = (N_T - N_T^*) \times \frac{dN_T}{dt}.$$

$$= (N_T - (\frac{\Lambda}{\mu R_0^T} + I_A^* B_C)) \times (\Lambda - \mu N_T - \delta_T I_A)$$

$$\leq (N_T - \frac{\Lambda}{\mu})(\Lambda - \mu N_T)$$

$$\leq -\frac{(\Lambda - \mu N_T)^2}{\mu} \leq 0, \quad (36)$$

since $I_A > 0$ and $R_0^T > 1$ at $E_T^*$.

Therefore, for $R_0^T > 1$, the EEP $E_T^*$ exists and $L_T$ is a strictly Lyapunov function. This implies that $E_T^*$ is globally asymptotically stable.

## 5. | Sensitivity Analysis of $R_e$

Sensitivity analysis enables the assessment of how each parameter within $R_e$ affects the transmission

and control dynamics of a disease. The normalized forward sensitivity index of $R_e$ relative to a parameter p is defined by Akinade and Afolabi (2020), and Bandekar and Ghosh (2022) as: $\Gamma_p^{R_e} = \frac{\partial R_e}{R_e} \div \frac{\partial p}{p}$. Since $R_e$ is the product of $R_0$ with a constant non-zero value, it suffices to say that:

$$\Gamma_p^{R_0} = \frac{\partial R_0}{\partial p} \times \frac{p}{R_0} \tag{37}$$

For the TB model, we recall from (4.2) that,

$$R_0^T = \frac{\Lambda\beta_T\rho_1(\mu+\omega_T)}{\mu(\rho_1+\mu)(\mu+\omega_T+\nu_T)(\delta_T+\gamma_T+\mu)}. \tag{38}$$

For $\Lambda$,
$$\Gamma_\Lambda^{R_0^T} = \frac{\partial R_0^T}{\partial \Lambda} \times \frac{\Lambda}{R_0^T}$$
$$= \frac{R_0^T}{\Lambda} \times \frac{\Lambda}{R_0^T} = 1.$$

For $\beta_T$,
$$\Gamma_{\beta_T}^{R_0^T} = \frac{\partial R_0^T}{\partial \beta_T} \times \frac{\beta_T}{R_0^T}$$
$$= \frac{R_0^T}{\beta_T} \times \frac{\beta_T}{R_0^T} = 1.$$

For $\rho_1$, $\frac{\partial R_0^T}{\partial \rho_1} = \frac{\Lambda\beta_T(\mu+\omega_T)}{\mu(\mu+\omega_T+\nu_T)(\delta_T+\gamma_T+\mu)} \times \frac{\partial D}{\partial \rho_1}$, (39)

where $D = \frac{\rho_1}{(\rho_1+\mu)}$.

By quotient rule of differentiation,

$$\frac{\partial D}{\partial \rho_1} = \frac{\mu}{(\rho_1+\mu)^2}.$$

Substituting this result in (39), we obtained;

$$\Gamma_{\rho_1}^{R_0^T} = R_0^T \times \frac{(\rho_1+\mu)}{\rho_1} \times \frac{\mu}{(\rho_1+\mu)^2} \times \frac{\rho_1}{R_0^T}$$
$$= \frac{\mu}{(\rho_1+\mu)}.$$

For $\omega_T$,
$$\frac{\partial R_0^T}{\partial \omega_T} = \frac{\Lambda\beta_T\rho_1}{\mu(\rho_1+\mu)(\delta_T+\gamma_T+\mu)} \times \frac{\partial D}{\partial \omega_T}, \tag{40}$$

where $D = \frac{(\mu+\omega_T)}{(\mu+\omega_T+\nu_T)}$.

By quotient rule of differentiation,
$$\frac{\partial D}{\partial \omega_T} = \frac{\nu_T}{(\mu+\omega_T+\nu_T)^2}.$$

Substituting this result in (40), we obtained;

$$\Gamma_{\omega_T}^{R_0^T} = R_0^T \times \frac{(\mu+\omega_T+\nu_T)}{(\mu+\omega_T)} \times \frac{\nu_T}{(\mu+\omega_T+\nu_T)^2} \times \frac{\omega_T}{R_0^T}$$
$$= \frac{\nu_T\omega_T}{(\mu+\omega_T)(\mu+\omega_T+\nu_T)}.$$

For $\nu_T$,

$$\frac{\partial R_0^T}{\partial \nu_T} = \frac{\Lambda\beta_T\rho_1(\mu+\omega_T)}{\mu(\rho_1+\mu)(\delta_T+\gamma_T+\mu)} \times \frac{\partial D}{\partial \omega_T}, \tag{41}$$

where $D = \frac{1}{(\mu+\omega_T+\nu_T)}$.

By quotient rule of differentiation,

$$\frac{\partial D}{\partial \nu_T} = -(\mu+\omega_T+\nu_T)^{-2}.$$

Substituting this result in (41), we obtained;
$$\Gamma_{\nu_T}^{R_0^T} = R_0^T \times (\mu+\omega_T+\nu_T) \times -(\mu+\omega_T+\nu_T)^{-2} \times \frac{\nu_T}{R_0^T}$$
$$= \frac{-\nu_T}{(\mu+\omega_T+\nu_T)}.$$

For $\gamma_T$, $\Gamma_{\gamma_T}^{R_0^T} = \frac{-\gamma_T}{(\mu+\gamma_T+\delta_T)}$.

For $\delta_T$,
$$\Gamma_{\delta_T}^{R_0^T} = \frac{-\delta_T}{(\mu+\gamma_T+\delta_T)}.$$

Lastly, for $\mu$, $\frac{\partial R_0^T}{\partial \mu} = \Lambda\beta_T\rho_1 \times \frac{\partial D}{\partial \mu}$, (42)

where $D = \frac{(\mu+\omega_T)}{\mu(\mu+\rho_1)(\mu+\omega_T+\nu_T)(\mu+\gamma_T+\delta_T)}$.

Let $V = \mu(\mu+\rho_1)(\mu+\omega_T+\nu_T)(\mu+\gamma_T+\delta_T)$,

$$\frac{\partial V}{\partial \mu} = \mu(\mu+\rho_1)(\mu+\omega_T+\nu_T) + \mu(\mu+\gamma_T+\delta_T)(2\mu+\rho_1$$
$$+\omega_T+\nu_T) + (\mu+\rho_1)(\mu+\omega_T+\nu_T)(\mu+\gamma_T+\delta_T)$$

$$\frac{\partial D}{\partial \mu} = \frac{V-(\mu+\omega_T)\frac{\partial V}{\partial \mu}}{V^2}.$$

Substituting this result in (42), we obtained;

$$\Gamma_\mu^{R_0^T} = R_0^T \times \frac{V}{(\mu+\omega_T)} \times \frac{\partial D}{\partial \mu} \times \frac{\mu}{R_0^T}$$
$$= \frac{(V-(\mu+\omega_T)\frac{\partial V}{\partial \mu})\mu}{V(\mu+\omega_T)}.$$

Substituting the parameter values in Table 2 into the sensitivity indices above, we obtained Table 3 below.

**Table 3** | Sensitivity Indices for the Basic Reproduction Number

| Parameters | Signs | **Values** |
|---|---|---|
| $\Lambda$ | + | 1 |
| $\beta_T$ | + | 1 |
| $\rho_1$ | + | 0.0038064 |
| $\omega_T$ | + | 0.8297130 |
| $\nu_T$ | - | 0.9882296 |
| $\gamma_T$ | - | 0.7628824 |
| $\delta_T$ | - | 0.2365526 |
| $\mu$ | - | 0.8458547 |

## 6. | Numerical Results and Discussion

The model's numerical solution was computed via the classical fourth-order Runge–Kutta scheme on MATLAB subroutine. The simulation utilizes parameter values provided in Table 2. The simulation was performed over a period of 80 weeks.

### 6.1 | Numerical Solution of the Model

Figures 3 to 7 are the graphical solution of the model's equations (1) to (5) respectively. Figure 3 is the susceptible population's trajectory. This class experienced a continuous and rapid decline in its population over a period of 10 weeks associated to progression into the latent class and especially into the vaccinated class as seen in Figures 4 and 7 respectively. Afterwards, the susceptible class maintained a stable value associated with an equivalent inflow into the population and outflow to other populations.

The latent TB infected class in Figure 4 experienced a decline in its population after the first 8 weeks indicating that its members were beginning to progress to active infectiousness thereby moving into the active TB infected class in Figure 5. Worthy of note is that the latent TB class, though approaches, didn't converge on zero indicating that the population remains non-empty. Increase in the active TB class lasted about 15 weeks after which it experienced a continuous de-population into the recovered class in Figure 6. The recovered class initially recorded a slow increase in its population for the first 5 weeks after which it experienced a considerably rapid increase.

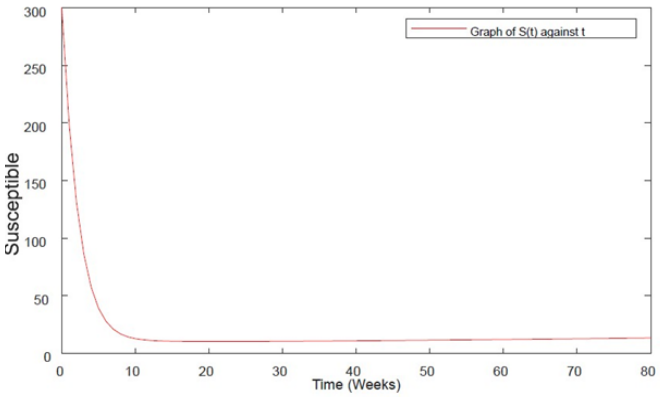


**Figure 3** | Susceptible TB Population Against Time

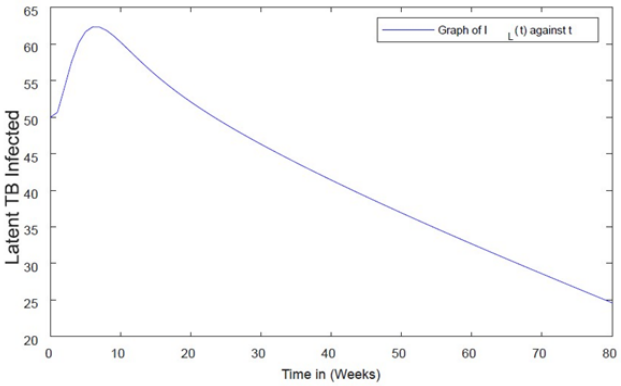


**Figure 4** | Latent TB Infected Population against Time

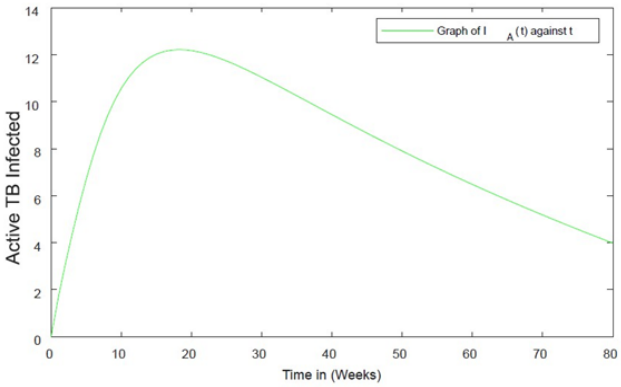


**Figure 5** | Active TB Infected Population against Time

After some time, however, This population is found to maintain a very slow increase in its population because of disease relapse. Same can't be said of

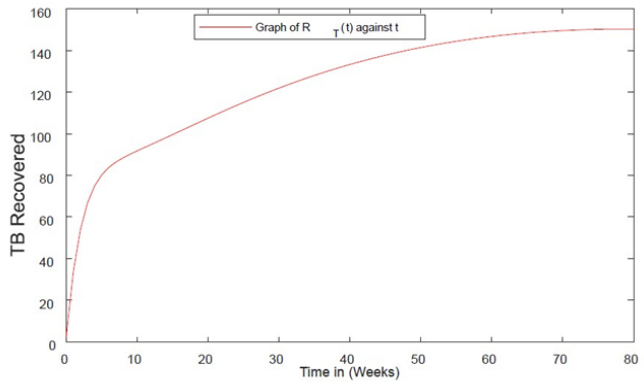


Figure 6: TB Recovered Population against Time

**Figure 6** | TB Receovered Population against Time

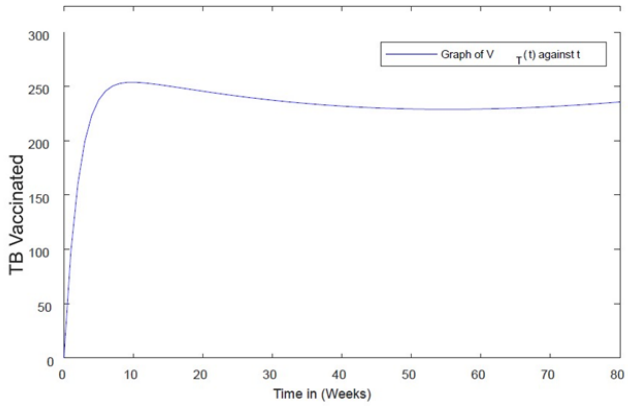


**Figure 7** | TB Vaccinated Population against Time

the vaccinated class which recorded a slight decline in its population after the first 10 weeks associated to the effect of immunity waning. Thereafter, this class maintained a stable value associated with an equivalence in inflow and outflow.

## 6.2 | Variation of Sensitive Parameters

Figure 8 depicts how variations in the vaccination rate influence the latent, active and vaccinated populations. Increasing the vaccination rate leads to a reduction in the latent and active infected classes and an associated increase in the vaccinated class. An increase in the treatment rate leads to a decrease in both the latent and active TB classes while the recovered class increases as seen in Figure 9. Figure 10 shows a slight increase in the population of the susceptible class and more significant increase in the latent and active TB classes as the rate of migration into the susceptible class increases. This suggests that increase in the population of the susceptible class results in a rapid spread of the disease.

The trajectories of effects of increase in disease relapse in Figure 11 show that the latent TB class initially experienced an increase in its population and then later a decrease. The susceptible class experience an increase in its population as the disease relapse rate increases while the recovered class experience a resultant decrease in its population. Figure 12 indicates a decline in the latent class and an increase in the active infected class as the progression rate from latent to active TB class increases.

The effect of loss of immunity of the vaccinated population in Figure 13 indicate an insignificant increase in the susceptible class as the latent and active TB populations continue to increase while the vaccinated class decreases. Lastly, the higher the TB contact/transmission rate the more the latent and infected TB classes grow and vice versa as shown in Figure 14.

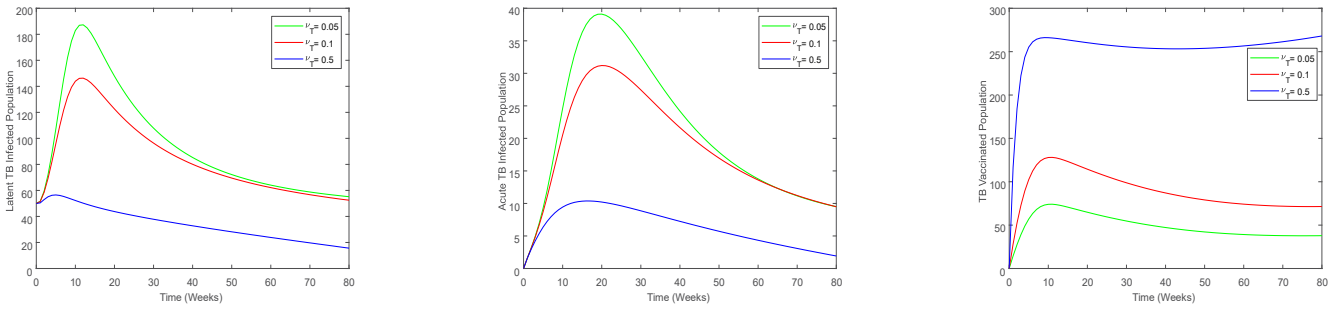


(a) Latent profile (b) Infected Profile (c) Vaccinated Profile

**Figure 8** | Effects of Vaccination Rate

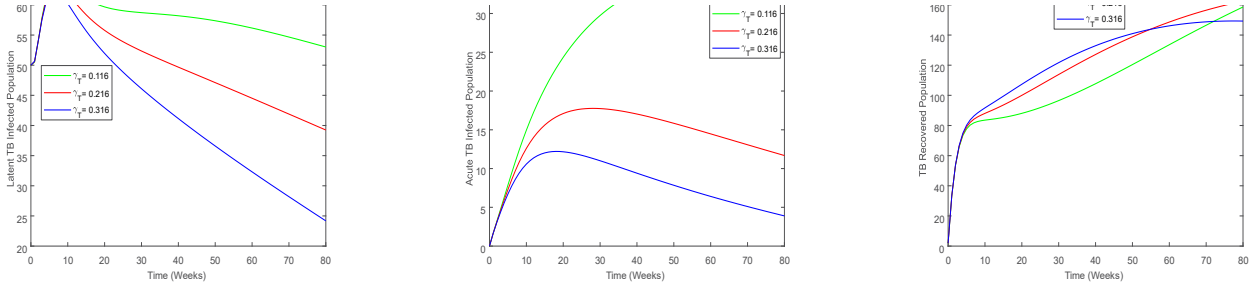


(a) Latent profile (b) Infected Profile (c) Recovered Profile

**Figure 9 |** Effects of Treatment Rate

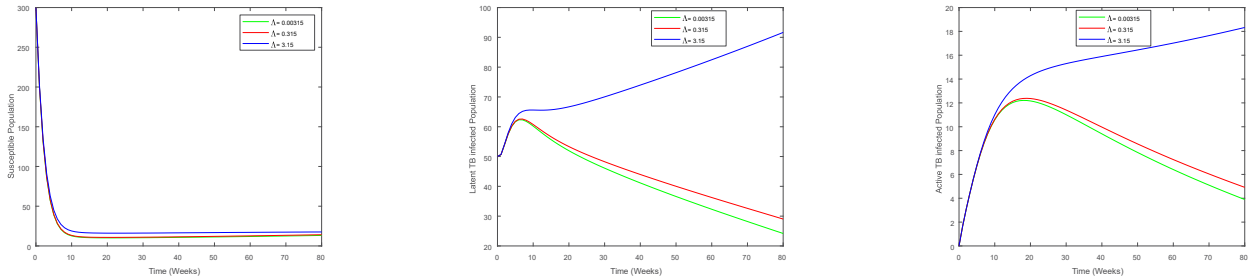


(a) Latent profile (b) Infected Profile (c) Recovered Profile

**Figure 10 |** Effects of Recruitment rate into the Susceptible population

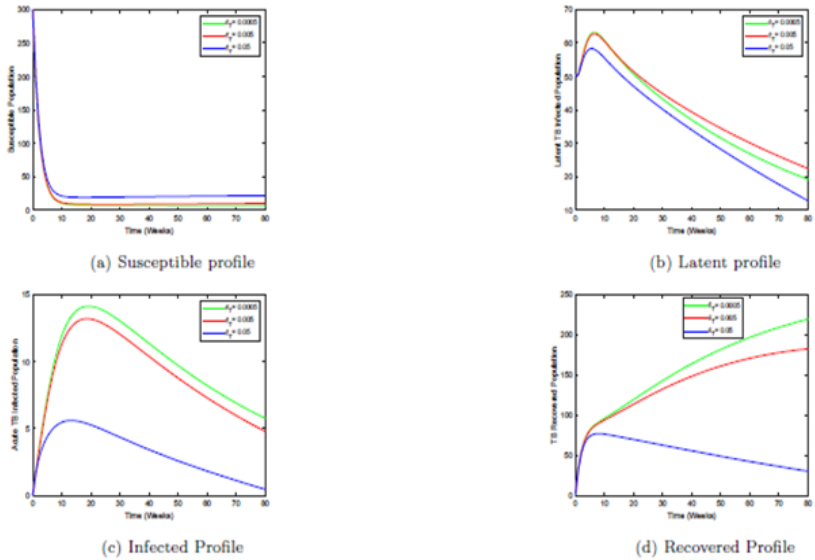

(a) Susceptible profile (b) Latent profile

(c) Infected Profile (d) Recovered Profile

**Figure 11 |** Effects of Disease Relapse

(a) Latent profile (b) Infected Profile

**Figure 12 |** Effects of Progression rate from latent to active TB

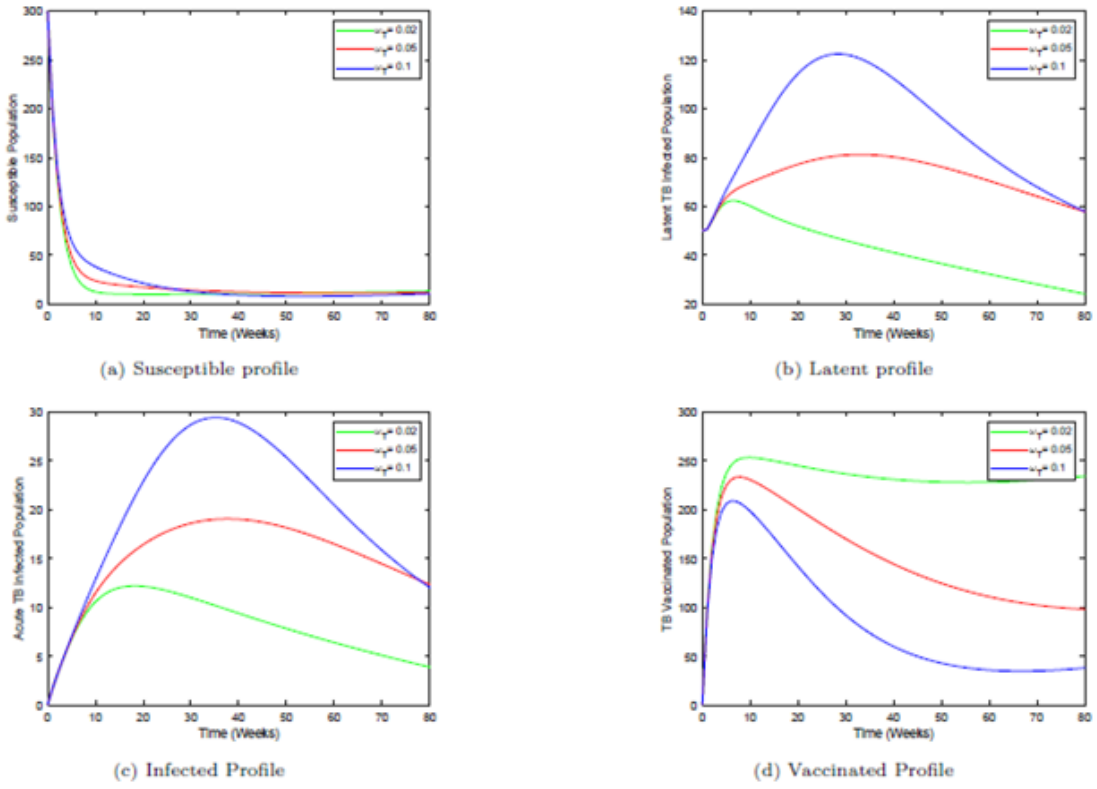


(a) Susceptible profile (b) Latent profile

(c) Infected Profile (d) Vaccinated Profile

**Figure 13 |** Effect of loss of Immunity after vaccination

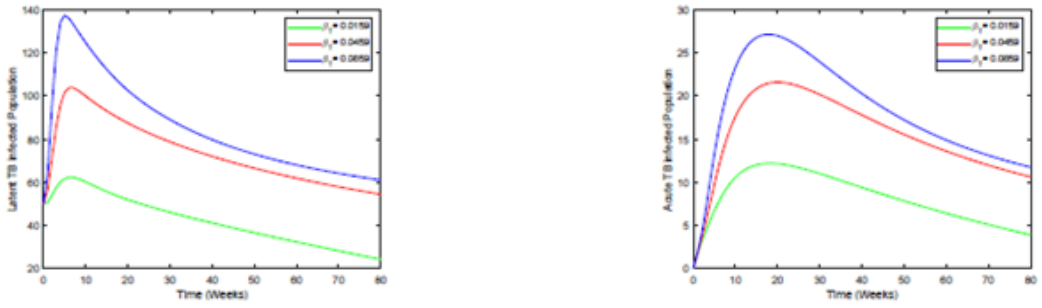


(a) Latent Profile (b) Infected Profile

**Figure 14 |** Effect of TB contact rate

## 7. | Conclusion

This work presents a novel, comprehensive deterministic model for modeling disease transmission, prevention and control dynamics of tuberculosis. The model was formulated as a system of 5 non-linear ordinary differential equations corresponding to 5 populations present in a tuberculosis endemic environment. Significant, yet previously overlooked, parameters such as disease relapse upon recovery, immunity wane after vaccination, The transition rate from latent TB infection to active disease, and treatment/recovery rate were notably considered in the formulation of this model.

Mathematical investigation of the model reveals that it possesses an invariant region, within which it is both epidemiologically and mathematically well-posed, and by applying the positivity theorem, we justified that the model's solution always remains non-negative. Further investigations show that the

model possesses a stable disease-free equilibrium point whenever the effective reproduction number, $R_e$, is less than 1, indicating that the disease can be curtailed and may not invade the population if the model with its properties is implemented. A unique endemic equilibrium point, which does not co-exist with the DFE, exists for the model whenever $R_e > 1$. This suggests that if the effective reproduction number is greater than one, the disease may remain endemic in such population.

Consequently, sensitivity analysis of $R_e$ was performed using the forward index sensitivity approach to obtain the specific rate of influence of parameters that affect the value of $R_e$. This analysis shows that the rate at which new individuals migrate into the susceptible population and transmission rate of tuberculosis are most sensitive to $R_e$ and will result in a rapid spread of the disease while vaccination and treatment rates are most sensitive to decrease its spread. Worthy of mention is the rate of immunity waning for the vaccinated class with sensitivity index of 0.8297130, indicating that 10% increase of this parameter will result in approximately 8.3% increase of $R_e$. We obtained the numerical solution of the model by applying the fourth-order Runge–Kutta scheme on MATLAB subroutine and various simulations of its parameters were discussed.

By and large, this research work was able to establish the effectiveness of mathematical modeling in predicting future trends and possible controls for tuberculosis. Consequent on the findings of this research, we recommend that awareness and sensitization be intensified, especially to people in tuberculosis endemic area, on how to reduce the transmission of this disease, possibly by proper hygiene e.g coughing/sneezing into the elbow, not staying in overcrowded areas with poor ventilation, etc.

Furthermore, we highly advocate for point of care diagnosis (POCD) of TB in endemic populations. This will reduce both its transmission and contact rates while enabling quick, easily accessible and accurate diagnosis of the disease, which should be followed with efficacious treatment. Moreover, not only must proper and adequate awareness be made on the potency of vaccination against tuberculosis, but also the possibility of attaining a vaccine with high efficacy, which possibly may result in a lifetime immunity against the disease (unlike BCG). The possibility of a treatment regime to completely remove tubercle bacilli, the causative agent of TB, thereby putting an end to cases of disease relapse upon recovery should also be considered.

To the scientific world, we recommend that an optimal control approach be implemented on the developed model to determine the best possible strategy or combination of strategies to minimize and ultimately end the disease spread, as the simulation results show that the TB infected population approaches but didn't converge on zero. The effect of the prevalence of other diseases on the Tuberculosis transmission and control dynamics should also be considered.

**Acknowledgment**

The authors acknowledge, with gratitude, the support of the Department of Mathematical Sciences of The Federal University of Technology Akure in providing a conducive for learning and research environment during the production of this manuscript.

**References**

Abu-Raddad, L. J., Sabatelli, L. J., Achterberg, T., Sugimoto, J. D., Longini, I. M., Dye, C. and Halloran, M. E. (2009) Epidemiological benefits of more-effective tuberculosis vaccines, drugs, and diagnostics. Proceedings of the National Academy of Sciences, 106 (33): 13980–13985.https://doi.org/10.1073/pnas.0901720106

Akinade, M. O., Afolabi, A. S. and Kimathi, M. E. (2019) Mathematical modeling and stability analyses of lassa fever disease with the introduction of the carrier compartment. Mathematical Theory and Modeling, 9 (6): 45–62. https://doi.org/10.7176/MTM

Akinade, M. O. and Afolabi, A. S. (2020) Sensitivity and stability analyses of a lassa fever disease model with control strategies. IOSR Journal of Mathematics (IOSR-JM), 16 (1): 29–42.

Ayinla, A. Y., Othman, W. A. M. and Rabiu, M. (2021) A mathematical model of the tuberculosis epidemic. Acta Biotheoretica, 1–31. https://doi.org/10.1007/s10441-020-09406-8

Baba, I. A., Yusuf, A., Nisar, K. S., Abdel-Aty, A. H. and Nofal T. A. (2021) Mathematical model to assess the imposition of lockdown during covid-19 pandemic, Results in Physics, 20: 103716. https://doi.org/10.1016/j.rinp.2020.103716

Bandekar, S. R. and Ghosh, M. (2022) A co-infection model on tb-covid-19 with optimal control and sensitivity analysis, Mathematics and Computers in Simulation, 200: 1–31. https://doi.org/10.1016/j.matcom.2022.04.001

Brown, C. W., Novotni, D. and Weber, A. (2006) Algorithmic methods for investigating equilibria in epidemic modeling. Journal of Symbolic Computation, 41 (11): 1157–1173. https://doi.org/10.1016/j.jsc.2005.09.011

Castillo-Chavez, C. and Song, B. (2004) Dynamical models of tuberculosis and their applications, Mathematical Biosciences & Engineering, 1 (2): 361–404.

Centers for Disease Control and Prevention (2024) Latent tb infection and tb disease. https://www.cdc.gov/tb/topic/basics/tbinfectiondisease.htm, 2024 (accessed 30 January 2024).

Colijn, C., Cohen, T. and Murray, M. (2009) Latent coinfection and the maintenance of strain diversity. Bulletin of mathematical biology, 71 (1): 247–263. https://doi.org/10.1007/s11538-008-9361-y

Diekmann, O., Heesterbeek, J. A. P. and Metz, J. A. (1990) On the definition and the computation of the basic reproduction ratio $r_0$ in models for infectious diseases in heterogeneous populations. Journal of mathematical biology, 28 (4): 365–382. https://doi.org/10.1007/BF00178324

Frith, J. (2014) History of tuberculosis; part 1-phthisis, consumption and the white plague, Journal of Military and Veterans Health, 22 (2): 29–35. https://search.informit.org/doi/10.3316/informit.430338287813994

Goletti, D., Matteelli, A., Cliff, J.M., Meintjes, G., Graham, S., Esmail, H. and Lee, S.S. (2025) World TB Day 2025 Theme "Yes! We Can End TB: Commit, Invest, Deliver" can be made a reality through concerted global efforts to advance diagnosis, treatment and research of tuberculosis infection and disease. International Journal of Infectious Diseases, Elsevier, 155: 1–3. https://doi.org/10.1016/j.ijid.2025.107892

Grace, A. G., Mittal, A., Jain, S., Tripathy, J. P., Satyanarayana, S., Tharyan, P. and Kirubakaran, R. (2019) Shortened treatment regimens versus the standard regimen for drug-sensitive pulmonary tuberculosis. Cochrane Database of Systematic Reviews, 12: 1–79. https://doi.org/10.1002/14651858.CD012918.pub2

Jajarmi, A., Ghanbari, B. and Baleanu, D. (2019) A new and efficient numerical method for the fractional modeling and optimal control of diabetes and tuberculosis co-existence. Chaos: An Interdisciplinary Journal of Nonlinear Science, 29 (9): 1–15. https://doi.org/10.1063/1.5112177.

Kim, S., Aurelio, A. and Jung, E. (2018) Mathematical model and intervention strategies for mitigating tuberculosis in the Philippines. Journal of theoretical biology, 443: 100–112. https://doi.org/10.1016/j.jtbi.2018.01.026

Kirschner, D., Pienaar, E. Marino, S. and Linderman, J. J. (2017) Review of computational and mathematical modeling contributions to our understanding of mycobacterium tuberculosis within-host infection and treatment. Current opinion in systems biology, 3: 170–185. https://doi.org/10.1016/j.coisb.2017.05.014

Koriko, O. and Yusuf, T. (2008) Mathematical model to simulate tuberculosis disease population dynamics. Journal of Applied Sciences, 5 (4): 301–306.

La Salle, J. P. (1976) The stability of dynamical systems. Society for Industrial and Applied Mathematics. https://epubs.siam.org/doi/pdf/10.1137/1.9781611970432.bm

Lofberg, J. (2004) Yalmip: A toolbox for modeling and optimization in matlab, Computer Aided Control Systems Design. IEEE international conference on robotics and automation (IEEE Cat. No. 04CH37508), 284–289. https://doi.org/10.1109/CACSD.2004.1393890

Mandal, S., Satyanarayana, S., McQuaid, F., Dodd, P. J., Menzies, N. A., White, R. G., Arinaminpathy, N., Houben, R. M., Dowdy, D. W., Smit, M. and Sahu, S. (2025) The global TB portfolio model: a tool for projecting the epidemiological impact of TB policy options. medRxiv, Cold Spring Harbor Laboratory Press, 1–23. https://doi.org/10.1101/2025.05.17.25327819

Mekonen, K. G. and Obsu, L. L. (2 022) Mathematical modeling and analysis for the co-infection of covid-19 and tuberculosis. Heliyon, 8 (10): 1–11. https://doi.org/10.1016/j.heliyon.2022.e11195

Mishra, B. K. and Srivastava, J. (2014) Mathematical model on pulmonary and multidrug-resistant tuberculosis patients with vaccination. Journal of the Egyptian mathematical Society, 22 (2): 311–316. https://doi.org/10.1016/j.joems.2013.07.006

Ogunmodimu, M. O., Enock, E. P., Kenyatta, A. P., Affognon, S. B. and Onwuegbuche F. C. (2024) A mathematical model for the prevention of hiv/aids in the presence of undetectable equals untransmittable viral load. International Journal of Mathematical Sciences and Optimization: Theory and Applications , 10 (2): 36–57. https://doi.org/10.5281/zenodo.10936948

Okafor, C. N., Rewane, A. and Momodu, I. I. (2023) Bacillus calmette guerin, StatPearls [Internet].

Owolabi, K. M. and Pindza, E. (2022) Nonlinear epidemic model for tuberculosis with caputo operator and fixed point theory. Healthcare Analytics, 2: 100–111. https://doi.org/10.1016/j.health.2022.100111

Pandey, S., Chadha, V., Laxminarayan, R. and Arinaminpathy, N. (2017) Estimating tuberculosis incidence from primary survey data: a mathematical modeling approach. The International Journal of Tuberculosis and Lung Disease, 21 (4): 366–374. https://doi.org/10.5588/ijtld.16.0182

Patterson, B. Morrow, C. Singh, V. Moosa, A., Gqada, M., Woodward, J., Mizrahi, V., Bryden, W., Call, C., Patel, S., Warner, D. and Wood, R. (2018) Detection of mycobacterium tuberculosis bacilli in bio- aerosols from untreated tb patients, Gates open research, 1 (11): 1–25. https://doi.org/10.12688/gatesopenres.12758.2

Rwezaura, H., Diagne, M., Omame, A., De-Espindola, A. L. and Tchuenche, J. M. (2022) Mathematical modeling and optimal control of sars-cov-2 and tuberculosis co-infection: a case study of Indonesia. Modeling Earth Systems and Environment, 8 (4): 5493–5520. https://doi.org/10.1007/s40808-022-01430-6

Sachdeva, K. S., Parmar, M., Rao, R., Chauhan, S., Shah, V., Pirabu, R., Balasubramaniam, D., Vadera, B., Anand, S., Mathew, M. and Solanki, H. (2020) Paradigm shift in efforts to end TB by 2025. Indian

Journal of Tuberculosis, Elsevier 67 (4): 48–60. https://doi.org/10.1016/j.ijtb.2020.11.001

Schluter, J. C., Sorensen, L., Bossert, A., Kersting, M., Staab, W. and Wacker B. (2021) Anticipating the impact of covid19 and comorbidities on the south african healthcare system by agent-based simulations. Scientific Reports, 11 (1): 1–9. https://doi.org/10.1038/s41598-021-86580-w

Tilahun, G. T., Makinde, O. D. and Malonza, D. (2018) Co-dynamics of pneumonia and typhoid fever diseases with cost effective optimal control analysis. Applied Mathematics and Computation, 316: 438–459. https://doi.org/10.1016/j.amc.2017.07.063

Trauer, J. M., Denholm, J. T. and McBryde, E. S. (2014) Construction of a mathematical model for tuberculosis transmission in highly endemic regions of the asia-pacific. Journal of theoretical biology, 358: 74–84. https://doi.org/10.1007/s10441-020-09406-8

Van-den-Driessche, P. and Watmough, J. (2002) Reproduction numbers and sub-threshold endemic equilibria for compartmental models of disease transmission. Mathematical biosciences, 180 (1-2): 29–48. https://doi.org/10.1016/S0025-5564(02)00108-6

Waaler, H., Geser, A. and Andersen, S. (1962) The use of mathematical models in the study of the epidemiology of tuberculosis. American Journal of Public Health and the Nations Health, 52 (6): 1002–1013.

White, P.J and Abubakar, I. (2016) Improving control of tuberculosis in low-burden countries: insights from mathematical modeling. Frontiers in microbiology, 7 (394): 1–8. http://dx.doi.org/10.3389/fmicb.2016.00394

World Health Organization (2023) Global tuberculosis report 2023, Geneva. World Health Organization. Licence: CC BY-NC-SA 3.0 IGO. ISBN 978-92-4-008385-1 (electronic version). ISBN 978-92-4-008386-8 (print version)

Wu, P., Lau, E. H., Cowling, B. J., Leung, C. C., Tam, C. M. and Leung, G. M. (2010) The transmission dynamics of tuberculosis in a recently developed chinese city. PloS one, 5 (5): 1–9. https://doi.org/10.1371/journal.pone.0010468

Yusuf, T. T. (2021) On global stability of disease-free equilibrium in epidemiological models. Journal of Mathematics and Statistics, 2 (3): 37–42. https://doi.org/10.24018/ejmath.2021.2.3.21